WAVEFORM SELECTION FOR RANGE AND DOPPLER ESTIMATION VIA BARANKIN BOUND SIGNAL-TO-NOISE RATIO THRESHOLD

John Kota, Narayan Kovvali, Daniel W. Bliss and Antonia Papandreou-Suppappola

School of Electrical, Computer, and Energy Engineering, Arizona State University, Tempe, Arizona

ABSTRACT

In this paper, we consider the tracking of a radar target with unknown range and range rate at low signal-to-noise ratio (SNR). For this nonlinear estimation problem, the Cramér-Rao lower bound (CRLB) provides a bound on an unbiased estimator's mean-squared error (MSE). However, there exists a threshold SNR at which the estimator variance deviates from the CRLB. We consider the Barankin bound (BB) on the range and range-rate variance in order to obtain a tighter lower bound at low SNR, and we use the BB to predict the SNR threshold for a transmitted signal. We demonstrate that the BB with the additional information provided by the threshold SNR has an advantage over the CRLB in selecting the optimal transmit waveform at low SNRs. We also develop a waveform parameter configuration method that uses the BB and the ambiguity function resolution cell measurement model to optimize the SNR threshold.

1. MOTIVATION AND RELATION TO PRIOR WORK

In narrowband radar and tracking problems, we are interested in simultaneously measuring the time delay and Doppler shift of a received target reflected signal for estimating the target's range and range rate [1]. The estimates of the target's location and velocity at the receiver can vary over time, partly due to the presence of clutter, environmental effects or general interference, and variance or resolution of these estimates can be affected by the choice of the transmitted waveform parameters [1–3]. Thus, techniques have been proposed to opportunistically transmit the best waveform [2, 3] in order to improve estimation error performance. Waveform configuration for low SNRs has also been considered with the track-before-detect algorithm and using the CRLB to predict estimates of the target's location and velocity [4, 5].

The CRLB provides a lower bound on an estimator's variance performance. However, in target tracking problems with the receiver operating under low SNR conditions, the CRLB may not provide a tight bound, leading to inaccurate predictions of the position and velocity estimates [1, 6–8]. For SNRs below a certain threshold SNR, the estimator variance deviates from the CRLB [6, 9]. As the SNR approaches this threshold region, the estimator's performance approaches an *ambiguity or threshold region*, where the estimator performance deteriorates rapidly. The errors in the threshold region are attributed to the fact that the estimator has dominant sidelobes due to unusually high noise fluctations. These fluctuations drive outlier values that are not, in general, the true values located at the mainlobe [1, 7, 10]

The Barankin bound (BB) is the greatest lower bound (infimum) on the variance of an unbiased parameter estimate [11]. The BB has been applied to many statistical signal processing problems to provide a tighter lower bound on the variance of an unbiased estimator. It also quantifies the threshold SNR, below which the BB starts to deviate from the CRLB [6, 9, 12–14]. As the BB requires the solution of an integral equation, it rarely has a closed form solution. However, computationally tractable approximations to the true BB have been considered for practical problems [10, 12, 13, 15–17].

The most common BB approximation was computed using the McAulay-Seidmann (MS) form [12, 14, 15]. In [8, 18], an approximation was considered that provides a tighter approximation than that of the MS form and is directly applicable to most signal processing measurement models. In [14], BB threshold analysis is performed for the track-before-detect problem using the MS approximation for Gaussian point-spread functions. In this paper, we employ the approximation introduced in [8] for the ambiguity function (AF) resolution cell measurement model [4, 5, 14] for a Gaussian-windowed linear frequency-modulated (LFM) chirp. We specifically examine the threshold SNR as a function of the waveform duration and frequency-modulation (FM) rate. We then propose a waveform parameter selection approach for low SNR target tracking based on the BB threshold SNR. Although for a different problem, a similar threshold SNR design approach was explored for acoustic array element spacing using the MS approximation in [10].

This paper is organized as follows. In Section 2, we provide the resolution cell measurement model and the Gaussian-windowed LFM signal characteristics. In Section 3, we obtain the BB approximation and we propose the optimal waveform selection for range and Doppler estimation based on the BB SNR threshold in Section 4. Estimation bound simulations are provided in Section 5.

2. RESOLUTION CELL MEASUREMENT MODEL

The AF resolution cell signal model can be written as [4, 5]

$$z^{(i,j)} = I_0 \, \mathrm{AF}_s(i\Delta_\tau, j\Delta_\nu; \mathbf{p}) + w^{(i,j)} \,, \tag{1}$$

for $i = 1, \dots N_\tau$, $j = 1, \dots N_\nu$. Here, I_0 is the return signal energy intensity, $s(t; \mathbf{p}) \in L^2(\mathbb{R})$ is the transmit waveform with parameter $\mathbf{p} \in \mathbb{R}^p$, and Δ_τ and Δ_ν are the delay and Doppler cell dimensions, respectively. The (i, j)th AF cell is defined in terms of the AF surface $\mathrm{AF}_s(\tau, \nu; \mathbf{p}) = | \int_{\mathbb{R}} s(t+\tau/2; \mathbf{p}) \, s^*(t-\tau/2; \mathbf{p}) \, e^{j2\pi\nu t} dt|^2$ [1]. The noise term $w^{(i,j)}$ in (1) is zero-mean, additive white Gaussian noise with variance σ_w^2. Note that the AF cell area is $\Delta_\tau \Delta_\nu$ and the total number of AF cells is $N_z = N_\tau N_\nu$, as demonstrated in Fig. 1. In vector form, (1) can be written as

$$\mathbf{z} = I_0 \, \mathbf{a}(\boldsymbol{\theta}, \mathbf{p}) + \mathbf{w} \,, \tag{2}$$

where $\boldsymbol{\theta} = [\tau \; \nu]^T$, $\mathbf{a}(\boldsymbol{\theta}, \mathbf{p}) \in \mathbb{R}^{N_z}$ is

$$\mathbf{a}(\boldsymbol{\theta}, \mathbf{p}) = [\mathrm{AF}_s(\Delta_\tau, \Delta_\nu; \mathbf{p}) \, \dots \, \mathrm{AF}_s(N_\tau \Delta_\tau, \Delta_\nu; \mathbf{p}) \dots$$
$$\dots \, \mathrm{AF}_s(\Delta_\tau, N_\nu \Delta_\nu; \mathbf{p}) \, \dots \mathrm{AF}_s(N_\tau \Delta_\tau, N_\nu \Delta_\nu; \mathbf{p})]^T \,,$$

This work was sponsored in part by DARPA under the SSPARC program. The views expressed are those of the authors and do not reflect the official policy or position of the Department of Defense or the U.S. Government.

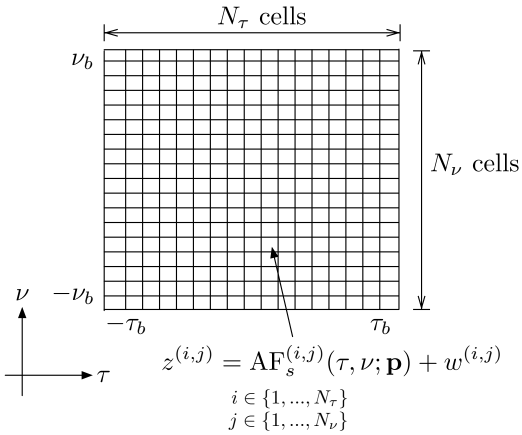

Fig. 1. AF resolution cell model for a $N_\tau \times N_\nu$ delay-Doppler grid, where $\mathrm{AF}^{(i,j)}(\tau, \nu; \mathbf{p}) = \mathrm{AF}_s(i\Delta_\tau, j\Delta_\nu; \mathbf{p})$.

and $\mathbf{w}$ is the white Gaussian noise vector. The vector $\boldsymbol{\theta}$ of deterministic parameters needs to be estimated to provide range $r = c\,\tau/2$ and range rate $\dot{r} = c\,\nu/(2f_c)$ measurements, where f_c is the carrier frequency and c is the signal propagation speed. Since the cells are assumed to be independent the AF resolution cell likelihood function is given by

$$p(\mathbf{z}|\boldsymbol{\theta}, \mathbf{p}) = \prod_{i=1}^{N_\tau} \prod_{j=1}^{N_\nu} p(z^{(i,j)}|\boldsymbol{\theta}, \mathbf{p})$$
$$= \frac{1}{(2\pi\sigma_w^2)^{N_z/2}} \exp\left[-\frac{1}{2\sigma_w^2} ||\mathbf{z} - I_0\, \mathbf{a}(\boldsymbol{\theta}, \mathbf{p})||_2^2\right] .$$

where $||\boldsymbol{v}||_2^2 = \boldsymbol{v}^T \boldsymbol{v}$ is the Euclidean norm.

We consider the Gaussian-windowed LFM signal of the form

$$s(t; \mathbf{p}) = (2\pi\lambda)^{-1/2} e^{-t^2/(2\lambda^2)} e^{j2\pi b_0 (t/t_r)^2} ,$$

where $\mathbf{p} = [b_0 \;\; \lambda]^T$, FM rate b_0, and Gaussian window duration λ. Note that we assume that all LFM signals have normalized unit energy. As the instantaneous frequency of the LFM signal is $2b_0 t$, its frequency range is $B = 2b_0\lambda$. Thus, if we fix the signal minimum and maximum bandwidth and duration, we can increase the bandwidth by increasing the LFM rate b_0.

The AF for the Gaussian-windowed LFM and its partial derivatives with respect to τ and ν (needed for computing estimation bounds) are given by [1]

$$\mathrm{AF}_s(\tau, \nu; \mathbf{p}) = \exp\left[-\frac{1}{2}\left(\tau^2/\lambda^2 + \lambda^2(\nu - 2b_0\tau)^2\right)\right] \quad (3)$$

$$\frac{\partial \mathrm{AF}_s(\tau, \nu; \mathbf{p})}{\partial \tau} = \frac{b_0\lambda^4(2\nu - 4b_0\tau) - \tau}{\lambda^2} \mathrm{AF}_s(\tau, \nu; \mathbf{p}) \quad (4)$$

$$\frac{\partial \mathrm{AF}_s(\tau, \nu; \mathbf{p})}{\partial \nu} = \lambda^2(2b_0\tau - \nu)\mathrm{AF}_s(\tau, \nu; \mathbf{p}) . \quad (5)$$

3. ESTIMATION BOUNDS

The CRLB is the weakest bound on the variance of an unbiased estimator as it does not offer accurate variance information for relatively low SNR and/or low data record lengths in estimation problems that exhibit the threshold SNR phenomenon. This is in contrast to the BB, which is the tightest bound on the variance of an unbiased estimator [11]. Note that the following relationship holds in general for the covariance matrix $\boldsymbol{\Sigma}_{\hat{\boldsymbol{\theta}}(\mathbf{z})}$ of a parameter estimate $\hat{\boldsymbol{\theta}}(\mathbf{z})$,

$$\boldsymbol{\Sigma}_{\hat{\boldsymbol{\theta}}(\mathbf{z})} \succeq \mathbf{BB} \succeq \mathbf{CRLB} ,$$

with equality asymptotic at high SNR and/or large data record lengths.

3.1. Barankin Bound Approximation

A new BB approximation is presented in [8], showing it to be a tighter approximation to the theoretical BB in comparison to the MS approximation [12, 15]. The approximated BB, $\mathbf{BB}(\boldsymbol{\Psi})$, with $\boldsymbol{\Psi} = (\boldsymbol{\theta}, \eta, \mathbf{p})$, is computed as

$$\mathbf{BB}(\boldsymbol{\Psi}) = \mathbf{V}^T \mathbf{G}(\boldsymbol{\Psi})^{-1} \mathbf{V} \quad (6)$$

where $\mathbf{V} = \left[\boldsymbol{\Delta} \; J(\boldsymbol{\theta}^{(0)}) \; \cdots \; J(\boldsymbol{\theta}^{(L)})\right]^T$,

$$\boldsymbol{\Delta} = \left[\mathbf{0}_{Q\times 1} \;\; \boldsymbol{\theta}^{(1)} - \boldsymbol{\theta}^{(0)} \;\cdots\; \boldsymbol{\theta}^{(L)} - \boldsymbol{\theta}^{(0)}\right] \quad \text{and}$$

$$\mathbf{G}(\boldsymbol{\Psi}) = \begin{bmatrix} \mathbf{MS}(\boldsymbol{\Psi}) & \mathbf{H}(\boldsymbol{\Psi})^T \\ \mathbf{H}(\boldsymbol{\Psi}) & \mathbf{EFI}(\boldsymbol{\Psi}) \end{bmatrix} .$$

Where η is the SNR, $\mathbf{MS}(\boldsymbol{\Psi}) \in \mathbb{R}^{(L+1)\times(L+1)}$ is the MS matrix, $\mathbf{EFI}(\boldsymbol{\Psi}) \in \mathbb{R}^{Q(L+1)\times Q(L+1)}$ is the extended Fisher information (EFI) matrix that extends the Fisher information matrix (FIM) to L test points $\boldsymbol{\theta}^{(l)} \in \boldsymbol{\Theta}$, $l = 1, \ldots L$, beyond the true parameter $\boldsymbol{\theta}^{(0)}$, $\mathbf{H}(\boldsymbol{\Psi}) \in \mathbb{R}^{Q(L+1)\times(L+1)}$ contains a mix of MS and EFI entries, and $J(\boldsymbol{\theta}^{(l)}) = \mathbf{I}_Q$, is the Jacobian of test point parameter vector; in our case, $\mathbf{I}_Q$ is the $Q \times Q$ identity matrix where $Q = 2$ for our signal model.

We apply the BB appropximation to $\mathbf{z} = I_0\mathbf{a}(\boldsymbol{\theta}, \mathbf{p}) + \mathbf{w}$, where $\mathbf{w}$ is a zero-mean white Gaussian noise vector with known covariance $\sigma_w^2 \mathbf{I}_{N_z}$. We evaluate the entries of the block matrices $\mathbf{MS}$, $\mathbf{EFI}$, and $\mathbf{H}$ in Eq. (6) for the Gaussian $\mathbf{z}$ as [8]

$$\mathbf{MS}_{m,n}(\boldsymbol{\Psi}_{m,n}) = \exp\left(\frac{I_0^2}{2\sigma_w^2}\left(a_{m,n}(\mathbf{p}) - \delta_{m,n}(\mathbf{p})\right)\right) \quad (7)$$

$$\mathbf{H}_i(\boldsymbol{\Psi}_{m,n}) = \frac{I_0^2}{\sigma_w^2} \mathbf{MS}_{m,n}(\boldsymbol{\Psi}_{m,n}) \frac{\partial \mathbf{a}^T(\boldsymbol{\theta}^{(m)}, \mathbf{p})}{\partial \boldsymbol{\theta}_i} \cdot \left(\mathbf{a}(\boldsymbol{\theta}^{(n)}, \mathbf{p}) - \mathbf{a}(\boldsymbol{\theta}^{(0)}, \mathbf{p})\right) \quad (8)$$

$$\mathbf{EFI}_{i,l}(\boldsymbol{\Psi}_{m,n}) = \frac{I_0^2\, \mathbf{MS}_{m,n}(\boldsymbol{\Psi}_{m,n})}{\sigma_w^2} \cdot \left\{ \frac{\partial \mathbf{a}^T(\boldsymbol{\theta}^{(m)}, \mathbf{p})}{\partial \boldsymbol{\theta}_i} \frac{\partial \mathbf{a}(\boldsymbol{\theta}^{(n)}, \mathbf{p})}{\partial \boldsymbol{\theta}_l} + \frac{I_0^2}{\sigma_w^2} \frac{\partial \mathbf{a}^T(\boldsymbol{\theta}^{(m)}, \mathbf{p})}{\partial \boldsymbol{\theta}_i} \left(\mathbf{a}(\boldsymbol{\theta}^{(n)}, \mathbf{p}) - \mathbf{a}(\boldsymbol{\theta}^{(0)}, \mathbf{p})\right) \cdot \left(\mathbf{a}(\boldsymbol{\theta}^{(m)}, \mathbf{p}) - \mathbf{a}(\boldsymbol{\theta}^{(0)}, \mathbf{p})\right)^T \frac{\partial \mathbf{a}(\boldsymbol{\theta}^{(n)}, \mathbf{p})}{\partial \boldsymbol{\theta}_l} \right\} \quad (9)$$

where $\boldsymbol{\Psi}_{m,n} = (\boldsymbol{\theta}^{(m)}, \boldsymbol{\theta}^{(n)}, \eta, \mathbf{p})$, $\boldsymbol{\theta}_i$ is the ith entry of $\boldsymbol{\theta}$ and

$$a_{m,n}(\mathbf{p}) = ||\mathbf{a}(\boldsymbol{\theta}^{(m)}, \mathbf{p}) + \mathbf{a}(\boldsymbol{\theta}^{(n)}, \mathbf{p}) - \mathbf{a}(\boldsymbol{\theta}^{(0)}, \mathbf{p})||_2^2$$
$$\delta_{m,n}(\mathbf{p}) = ||\mathbf{a}(\boldsymbol{\theta}^{(m)}, \mathbf{p})||_2^2 + ||\mathbf{a}(\boldsymbol{\theta}^{(n)}, \mathbf{p})||_2^2 - ||\mathbf{a}(\boldsymbol{\theta}^{(0)}, \mathbf{p})||_2^2 .$$

Here, SNR is defined as $\eta = I_0^2/\sigma_w^2$, $m, n \in \{0\} \cup \{1, \ldots, L\}$ are indexed up to the maximum number of test points L (including the true parameter $\boldsymbol{\theta}^{(0)}$) and $i, l \in \{1, \ldots, Q\}$ are indexed up to the dimension Q of $\boldsymbol{\theta}$. Note that for $L = 1$, the BB becomes the Hammersley-Chapman-Robbins bound (HChRB) [8, 14].

3.2. Barankin Bound Test Point Selection

The BB holds for any test point $\boldsymbol{\theta}^{(l)} \in \boldsymbol{\Theta}$ provided that the point is inside the parameter space for the given problem [8, 13, 15, 19].

For the resolution cell model, the parameter space $\mathbf{\Theta}$ has support on $[-\tau_b, \tau_b] \times [-\nu_b, \nu_b]$, and we choose the test points to be the boundary corners of the parameter space. This is because the boundary reflects a maximum outlier in the parameter space and thus was found to maximize the BB on $\mathbf{\Theta}$. We continue to increased the number of test points L until there was no significant gain in tightness of the bound. As an example, Fig. 2 shows the BB approximation for an increasing number of test points for an LFM with $B = 1$ MHz and $\lambda = 1$ μs on a 500×500 grid.

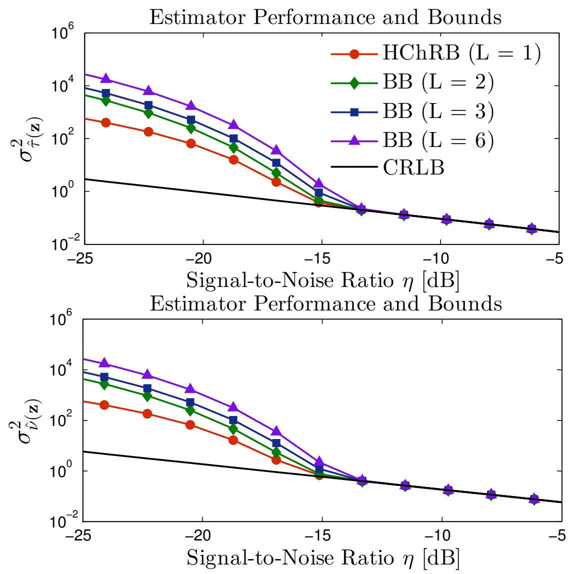

Fig. 2. Performance bounds: CRLB, Hammersley-Chapman-Robbins bound (HChRB) which is the BB bound with $L = 1$ test points, and BB for an increasing number of test points.

Note that the CRLB can be computed with the true parameter $\boldsymbol{\theta}^{(0)}$ using only the FIM. It is computed directly from the BB approximation explicitly in terms of $\mathbf{a}(\boldsymbol{\theta}, \mathbf{p})$ as

$$\mathbf{CRLB}(\eta, \mathbf{p}) = \mathbf{EFI}_{1,1}(\mathbf{\Psi}_{0,0})^{-1}$$

$$= \eta^{-1} \begin{bmatrix} \frac{\partial \mathbf{a}^T(\boldsymbol{\theta}^{(0)},\mathbf{p})}{\partial \tau} \frac{\partial \mathbf{a}(\boldsymbol{\theta}^{(0)},\mathbf{p})}{\partial \tau} & \frac{\partial \mathbf{a}^T(\boldsymbol{\theta}^{(0)},\mathbf{p})}{\partial \tau} \frac{\partial \mathbf{a}(\boldsymbol{\theta}^{(0)},\mathbf{p})}{\partial \nu} \\ \frac{\partial \mathbf{a}^T(\boldsymbol{\theta}^{(0)},\mathbf{p})}{\partial \nu} \frac{\partial \mathbf{a}(\boldsymbol{\theta}^{(0)},\mathbf{p})}{\partial \tau} & \frac{\partial \mathbf{a}^T(\boldsymbol{\theta}^{(0)},\mathbf{p})}{\partial \nu} \frac{\partial \mathbf{a}(\boldsymbol{\theta}^{(0)},\mathbf{p})}{\partial \nu} \end{bmatrix}^{-1}.$$

4. WAVEFORM SELECTION ALGORITHM

Recalling that the BB is asymptotically equivalent to the CRLB for high SNR values, as visualized in Fig. 3(c), we formally define the threshold SNR η_{th} to be the value at which the BB estimator variance appreciably deviates from the respective CRLB. At high SNR, the relative error between the BB and CRLB is within some $\epsilon > 0$. We define this asymptotic SNR region as the set $\mathcal{A}_\epsilon(\mathbf{p}) = \{\eta \in \mathbb{R}_+ : \rho(\eta, \mathbf{p}) < \epsilon\} \subset \mathbb{R}$, where $\rho(\eta, \mathbf{p})$ is the relative deviation of the BB from the CRLB and is given by

$$\rho(\eta, \mathbf{p}) = \frac{\text{trace}\{\mathbf{BB}(\mathbf{\Psi}) - \mathbf{CRLB}(\mathbf{\Psi})\}}{\text{trace}\{\mathbf{CRLB}(\mathbf{\Psi})\}}.$$

Therefore, the value of η where $\rho(\eta, \mathbf{p})$ is a maximum represents the BB threshold SNR. Thus, we compute the threshold SNR as

$$\eta_{\text{th}}(\mathbf{p}) = \arg \max_{\mathcal{A}_\epsilon(\mathbf{p})} \rho(\eta, \mathbf{p}). \tag{10}$$

It can be clearly seen in Eq. (10), the threshold SNR depends on the choice of the waveform parameters $\mathbf{p}$. As a result, we can consider using the knowledge of a signal's threshold SNR for selecting a transmit waveform $s(t; \mathbf{p})$ that is suitable for the current tracker SNR that may be varying during tracking due to clutter or interference.

5. SIMULATIONS

We computed the AF cells using with $N_\tau = 500$, $N_\nu = 500$ for time delay and Doppler, respectively, with supports $[-30, 30]$ μs and $[-30, 30]$ MHz. Fig. 3(a) shows $\rho(\eta, \mathbf{p})$ for a fixed bandwidth $B = 1$ MHz for various durations between $0.1 \le \lambda \le 10\mu s$ resulting in a waveform parameter vector $\mathbf{p} = [\lambda \; 0.5/\lambda]^T$. Here, the FM rate is given by $0.5/\lambda$ in MHz^2. We have plotted $\eta_{\text{th}}(\mathbf{p})$ as a function of duration in Fig. 3(b) for when $\epsilon = 10^{-1}$. We see that there is a peak in the threshold SNR around 1 μs. This is where the AF is most localized in both time delay and Doppler shift for this particular parameter space.

For this case we find that, the more spread the AF is in the parameter space, the lower the threshold SNR is. However, for target tracking performance, this also means decreased range and range rate resolution given by the relationships in Eqs. (11)-(12) for the Gaussian-windowed LFM as [1]

$$\sigma_r = \frac{c}{2}\left(\frac{1}{\lambda^2} + 4b_0^2\lambda^2\right)^{-1/2} \tag{11}$$

$$\sigma_{\dot{r}} = \frac{c}{2f_c\lambda}. \tag{12}$$

Thus, we find that there is a trade off to be considered between a signal's η_{th} and its ability to resolve a target's location and velocity.

Using the same AF grid with $N_\tau = 500$, $N_\nu = 500$ and support $[-30, 30]$ μs and $[-30, 30]$ MHz, we show $\rho(\eta, \mathbf{p})$ in Fig. 4(a) for an LFM signal with a fixed duration $\lambda = 1$ μs and varying the FM rate b_0, thus we have a parameter vector $\mathbf{p} = [1\mu s \;\; b_0]^T$. The corresponding values of $\eta_{\text{th}}(\mathbf{p})$ as a function of FM rates, for $0.1 \le b_0 \le 10$ THz^2, is shown in Fig. 4(b) with $\epsilon = 10^{-1}$. Note that the values of the chirp rate here are chosen as a simulation example to show general behaviour and that practical radar waveform specifications may be different.

We see that the threshold SNR decreases as the LFM rate b_0. We do not find that η_{th} reaches a peak as it did for the previous example and intuitively this result makes sense due to the fact that the chirp rate will only affect the range resolution whereas in the previous example we can see the duration affects both the range and range rate resolution as can be seen in Eqs. (11)-(12).

6. CONCLUSION

In this paper, we used an approximation of the BB for Gaussian windowed LFM signals with the AF resolution cell measurement model to compute a tigher lower bound for range and Doppler estimation. We proposed a waveform selection algorithm based on the BB threshold SNR, and we investigated the threshold SNR as a function of LFM rate for a fixed duration and a a function of fixed bandwidth and variable signal duration. With these results, we introduce an approach of computing the threshold SNR based of the rate and duration of the LFM signal using the BB and CRLB bounds.

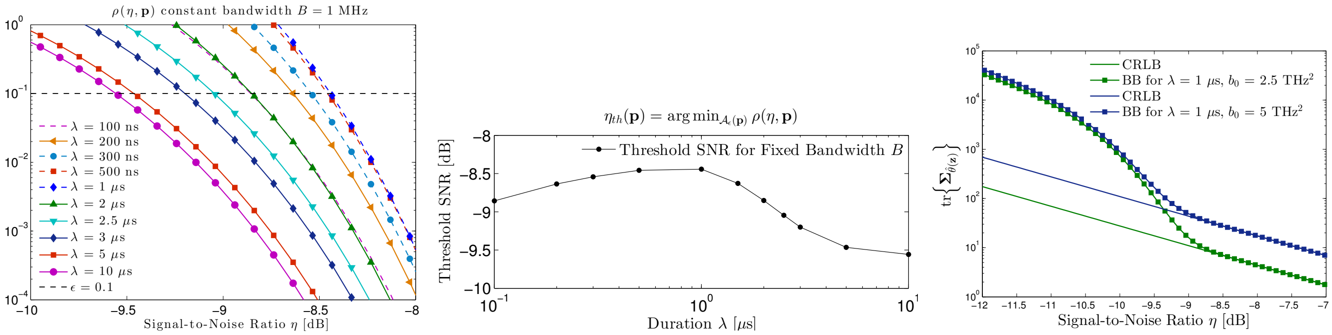

(a) (b) (c)

Fig. 3. (a) Relative CRLB and BB deviation $\rho(\eta, \mathbf{p})$ for fixed bandwidth $B = 1$ MHz and varying LFM duration λ; (b) Threshold SNR $\eta_{th}(\mathbf{p})$ for fixed bandwidth $B = 1$ MHz and LFM duration $0.1 \leq \lambda \leq 10$ μs; (c) CRLB and BB for fixed duration $\lambda = 1$ μs and varying LFM rate b_0.

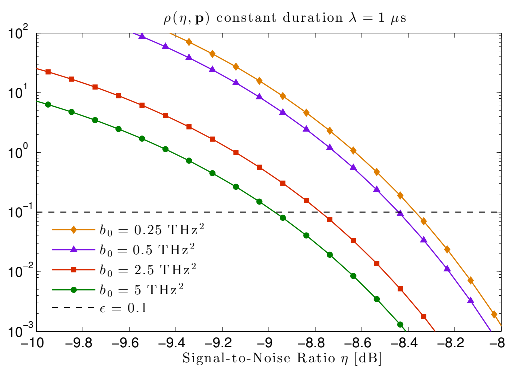

(a)

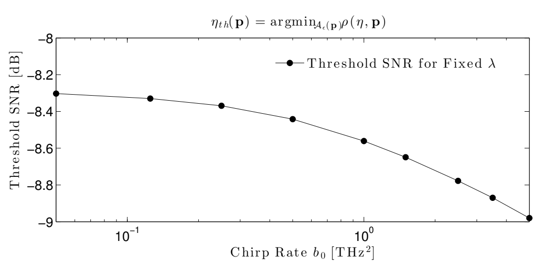

(b)

Fig. 4. (a) CRLB and BB relative deviation $\rho(\eta, \mathbf{p})$ for an LFM signal with fixed duration $\lambda = 1$ μs and varying FM rate b_0; (b) Threshold SNR $\eta_{th}(\mathbf{p})$ for an LFM signal with fixed duration $\lambda = 1$ μ and FM rate $0.1 \leq b_0 \leq 10$ THz^2.

7. REFERENCES

[1] H. L. V. Trees, *Detection, Estimation, and Modulation Theory, Radar-Sonar Signal Processing and Gaussian Signals in Noise*. Wiley-Interscience, October 2001, vol. III.

[2] S. P. Sira, Y. Li, A. Papandreou-Suppappola, D. Morrell, D. Cochran, and M. Rangaswamy, "Waveform-agile sensing and processing," *Signal Processing Magazine*, vol. 26, no. 1, pp. 53–64, January 2009.

[3] S. P. Sira, A. Papandreou-Suppappola, and D. Morrell, "Dynamic configuration of time-varying waveforms for agile sensing and tracking in clutter," *IEEE Transactions on Signal Processing*, vol. 55, no. 7, pp. 3207–3217, July 2007.

[4] J. J. Zhang, Q. Ding, S. Kay, A. Papandreou-Suppappola, and M. Rangaswamy, "Agile multi-modal tracking with dependent measurements," in *Asilomar Conference on Signals, Systems, and Computers*, November 2010, pp. 1653–1657.

[5] S. Liu, S. Bhat, J. J. Zhang, Q. Ding, R. Narayanan, A. Papandreou-Suppappola, S. Kay, and M. Rangaswamy, "Design and performance of an integrated waveform-agile multi-modal track-before-detect sensing system," in *Asilomar Conference on Signals, Systems, and Computers*, November 2011, pp. 1530–1534.

[6] L. Knockaert, "The barankin bound and threshold behavior in frequency estimation," *IEEE Transactions on Information Theory*, vol. 45, no. 9, pp. 2398–2401, August 1997.

[7] H. L. V. Trees, *Bayesian Bounds for Parameter Estimation and Nonlinear Filtering/Tracking*. Wiley-IEEE Press, August 2007.

[8] E. Chaumette, J. Galy, A. Quinlan, and P. Larzabal, "A new barankin bound approximation for the prediction of the threshold region performance of maximum likelihood estimators," *IEEE Transactions on Signal Processing*, vol. 56, no. 11, pp. 5319–5333, November 2008.

[9] A. Zeira and P. M. Schultheiss, "Realizable lower bounds for time delay estimation: Part 2 - threshold phenomena," *IEEE Transactions on Signal Processing*, vol. 42, no. 5, pp. 1001–1007, May 1994.

[10] T. Li, J. Tabrikian, , and A. Nehorai, "A barankin-type bound on direction estimation using acoustic sensor arrays," *IEEE Transactions on Signal Processing*, vol. 59, no. 1, pp. 431–435, January 2011.

[11] E. W. Barankin, "Locally best unbiased estimates," *The Annals of Mathematical Statistics*, vol. 20, no. 4, pp. 447–501, December 1949.

[12] A. Pinkus and J. Tabrikian, "Barankin bound for range and doppler estimation using orthogonal signal transmission," in *IEEE Conference on Radar*, April 2006.

[13] J. Tabrikian and J. L. Krolik, "Barankin bounds for source localization in an uncertain ocean environment," *IEEE Transactions on Signal Processing*, vol. 47, no. 11, pp. 2917–2927, November 1999.

[14] M. Morelande and B. Ristic, “Signal-to-noise ratio threshold effect in track before detect,” *IET Radar, Sonar & Navigation*, vol. 3, no. 6, pp. 601–608, April 2009.

[15] R. J. McAulay and L. P. Seidman, “A useful form of the barankin lower bound and its application to LFM threshold analysis,” *IEEE Transactions on Information Theory*, vol. 15, no. 2, pp. 273–278, March 1969.

[16] J. S. Abel, “A bound on mean-square-estimate error,” *IEEE Transactions on Information Theory*, vol. 39, no. 5, pp. 1675–1680, September 1993.

[17] K. Todros and J. Tabrikian, “General classes of performance lower bounds for parameter estimation - Part I: Non-bayesian bounds for unbiased estimators,” *IEEE Transactions on Information Theory*, vol. 56, no. 10, pp. 5045–5063, October 2010.

[18] A. Quinlan, E. Chaumette, and P. Larzabal, “A direct method to generate approximations of the barankin bound,” in *IEEE International Conference on Acoustic, Speech, and Signal Processing (ICASSP)*, vol. 3, 2006, pp. 1520–6149.

[19] L. N. Atallah, J.-P. Barbot, and P. Larzabal, “From chapman-robbins bound towards barankin bound in threshold behaviour prediction,” *IEEE Electronic Letters*, vol. 40, no. 4, pp. 279–280, February 2004.